

PACS numbers: 42.55.Rz; 42.70.Hj; 42.60.Lh
DOI: 10.1070/QE2006v036n07ABEH013185

Active laser media based on fianite crystals

Yu.K. Voron'ko, E.E. Lomonova, V.V. Osiko, A.A. Sobol', S.N. Ushakov, V.E. Shukshin

Abstract. **The spectral and lasing parameters of Yb^{3+} ions in zirconium dioxide crystals with a stabilised cubic structure (fianites) are studied. It is found that the absorption and luminescence spectra of Yb^{3+} in these crystals are characterised by a considerable inhomogeneous broadening. The nature of this broadening is investigated and the model of optical centres consistent with the properties of the inhomogeneous spectra of Yb^{3+} in the cubic zirconium dioxide crystal is proposed. It is shown that fianites can be used in solid-state lasers. Lasing in Yb^{3+} ions in diode-pumped fianite crystals was obtained and studied.**

Keywords: *solid-state lasers, fianites, spectroscopy*.

1. Introduction

The development of diode-pumped tunable femtosecond lasers is a problem of current interest in laser physics. Within the framework of this problem, the search is now underway for new laser media with spectral properties appropriate for generating tunable ultrashort pulses.

Zirconium dioxide crystals have a number of unique properties that favour their applications in a variety of technical fields. These materials offer a unique combination of physical and chemical properties: high mechanical characteristics (high durability and strength) and stability to the action of most chemical reagents, ionising radiations, and high temperatures. The number of studies devoted to the properties, crystal structure, and special applications of zirconium dioxide crystals achieves a few tens of papers every year.

A specific feature of these materials is that the most interesting crystals of cubic structure can exist at room temperature only if they are stabilised by oxides CaO, MgO, Y_2O_3, and a number of rare-earth oxides. The structure of ZrO_2 is such that during synthesis from melts, unstabilised zirconium dioxide undergoes two polymorphic transitions upon cooling, one of which (tetragonal → monoclinic) is accompanied by a considerable change in the crystal volume, resulting in the destruction of single crystals.

Transparent zirconium dioxide crystals of cubic structure (fianites) suitable for lasers can be synthesised at certain concentrations of stabilising oxide. Thus, yttrium oxide at the molar concentration 10 % – 33 % is often used as a stabiliser for fianites.

Therefore, only activated crystals with the cubic structure and chemical composition ZrO_2 – (10 % – 20 %) Y_2O_3 (TR_2O_3) can be used in lasers. In this composition, due to the heterovalent replacement of Zr^{4+} ions by Y^{3+} ions, one oxygen vacancy is formed per each two introduced Y^{3+} ions. The presence of vacancies in a stabilised zirconium dioxide crystal leads to the disordering of the crystal lattice, resulting in a considerable inhomogeneous broadening of the spectral lines of activating ions. Disordered crystals with broad inhomogeneous absorption and luminescence spectra of activating ions have the following advantages over single crystals with a regular crystal lattice:

(i) The possibility of tuning laser radiation within a broad inhomogeneous luminescence band whose width can achieve a few tens of nanometres;

(ii) the possibility of generating ultrashort pulses;

(iii) better thermal and mechanical parameters compared to those of commercial laser glasses;

(iv) high stability to external actions and the temperature drift of the pump wavelength;

(v) the possibility of a broad choice of activating ions.

The spectroscopic properties and lasing possibilities of fianite crystals doped with rare-earth ions (TR^{3+}) have not been adequately investigated. It is known that the spectroscopic properties of activating ions in dielectric laser crystals considerably depend on the composition and structure of the coordinating environment of these ions.

Any crystal contains a set of optical centres whose composition, local symmetry, and relative concentration depend on the crystal nature, the total concentration of activators, crystal growth technology, annealing, etc. The distribution of optical TR^{3+} centres in crystals of stabilised zirconium dioxide (with the concentration of Y_2O_3 equal to 10 % – 20 %) will be determined first of all by the concentration of stabilising ions (Y^{3+}) and oxygen vacancies.

We studied the spectral properties of activating ions and estimated the possibility of using $ZrO_2 - Y_2O_3$ crystals as laser matrices by the example of the Yb^{3+} ion which offers a number of advantages over other rare-earth ions. These advantages are:

(i) A simple energy level diagram excluding cross-relaxation, up-conversion, and excited-state absorption;

Yu.K. Voron'ko, E.E. Lomonova, V.V. Osiko, A.A. Sobol', S.N. Ushakov, V.E. Shukshin A.M. Prokhorov General Physics Institute, Russian Academy of Sciences, ul. Vavilova 38, 119991 Moscow, Russia; e-mail: osiko@lst.gpi.ru, lomonova@lst.gpi.ru, ushakov@lst.gpi.ru

Received 3 April 2006
Kvantovaya Elektronika **36** (7) 601 – 608 (2006)
Translated by M.N. Sapozhnikov

(ii) a small Stokes shift (which is especially important for the activation of disordered crystals whose thermal properties are inferior to those of ordered media);

(iii) the possibility of pumping by InGaAs or InAlGaAs diodes because the absorption band of the Yb^{3+} ion lies in the 930–980-nm range overlapped by the tuning range of these diodes [1].

2. Crystal structure and physical properties of fianites

In 1971, single crystals of cubic zirconium dioxide $ZrO_2 - Y_2O_3$ solid solutions were synthesised at Lebedev Physics Institute, Academy of Sciences of USSR. The study of physical properties of these single crystals [2] is of great interest because they combine a high hardness with good optical characteristics such as the isotropic structure, a broad transparency band, and the possibility of doping with various impurities in a broad concentration range. These crystals were called fianites in honour of Lebedev Physics Institute [from FIAN (Fizicheskii Institut Akademii Nauk) in Russian], where they were first synthesised and investigated in detail.

Fianite crystals with a cubic symmetry are isotropic and have a high radiation resistance and chemical stability, a high heat conduction, and are transparent in a broad spectral range from 250 to 7500 nm. They may be doped in a broad concentration range with trivalent and tetravalent rare-earth ions, elements of the iron group (V, Cr, Mn) and by other transition group elements. Fianites can be grown in large amounts (tens of kilograms) during one technological cycle.

The spectroscopic properties of stabilised zirconium dioxide crystals activated with rare-earth ions considerably differ from those of many laser materials with the ordered structure (for example, YAG laser crystals). These crystals have optical properties that are similar to the properties of other disordered media.

Because the concentration of stabilising trivalent oxides required for obtaining high-optical quality single crystals not subjected to phase transitions lies within 10 %–33 %, any laser crystals based on ZrO_2 have a high initial concentration of oxygen vacancies producing the local deformations of the crystal lattice. As a result, the activating ions in the crystal lattice have different environments, which leads to noticeable differences in their individual optical spectra and broadening of the total spectrum. The structure disordering and, therefore, the inhomogeneous broadening increase due to distortions of remote coordination spheres. The presence of broad absorption and luminescence bands in activated fianite crystals allows one to use all the advantages of disordered crystals.

The growth technology of fianites, their crystal structure, phase transitions, mechanical, optical, and other properties are described in monographs [3–5].

3. Structure and composition of the coordination spheres of ions stabilising fianites

The structure and composition of the environment of impurity ions in fianite crystals are considered in [6]. As shown above, the cubic phase of zirconium dioxide was stabilised by replacing Zr^{4+} ions by Y^{3+} ions. In this case, the structure and composition of the environment of impurity Y^{3+} or TR^{3+} ions are mainly determined by the following factors. Because the yttrium ion replacing Zr^{3+} and the oxygen vacancy are point defects with the effective charges −1 and +2, respectively, their Coulomb interaction assumes the location of vacancies predominantly in the first coordination sphere in oxygen [the nearest neighbour (NN) position of the Y^{3+} (TR^{3+}) ion]. On the other hand, the Zr^{4+} ion with a small radius tends to the seven-fold coordination, as in the case of the stable monoclinic phase of zirconium dioxide. Therefore, the zirconium ion tends to have vacancies in its nearest environment, leaving the eight-fold oxygen coordination for the Y^{3+} ion. Then, the oxygen vacancy is located in the second coordination sphere [the next nearest neighbour position (NNN)] with respect to the Y^{3+} ion. These two factors, acting in the opposite directions, are decisive in the distribution of stabilising ions. This distribution can also depend on a number of second-order factors such as the association of vacancies of stabilising ions, the possibility of formation of clusters of stabilising ions, etc.

At present there is no general agreement among researchers regarding the environment of Y^{3+} (TR^{3+}) ions in $ZrO_2 - Y_2O_3$ crystals at concentrations of Y_2O_3 11 %–18 %. Based on the neutron diffraction analysis of these crystals, the authors of paper [7] concluded that Y^{3+} is located in the NN position with respect to a vacancy, whereas the authors of paper [8], who used, in particular, the EXAFS method, assumed that Y^{3+} is located in the NNN position with respect to vacancies. The theoretical calculations of the structure of cubic stabilised zirconium oxide [9] showed that the location of vacancies for Y^{3+} ion is preferable in the second coordination sphere. The location of vacancies and the probable coordination of Zr^{4+}, Y^{3+}, and R^{3+} ions in stabilised zirconium dioxide crystals are also reported in [9].

It was shown in [10] that the compensation mechanism of the inconsistence between the radii of a lattice cation and an impurity ion and, hence, the distribution of oxygen vacancies is very specific for various TR^{3+} ions. Concerning the properties of the structure and composition of the corresponding optical centres, we can assert that, if a stabilising (activating) ion has an oxygen vacancy in the first coordination sphere (in the NN position), it is located at the centre of a seven-pointed star in the field of trigonal symmetry. The interaction of this ion with ions in the next coordination spheres gives rise to numerous optical centres with the structure and crystal fields weakly differing from the base ones, which results in the broadening of the spectral lines of the luminescence centres of the first base configuration.

If the oxygen vacancy is not located in the nearest coordination sphere of Y^{3+} (TR^{3+}), the impurity ion is located at the centre of an eight-pointed star and its crystalline field should have the cubic (or tetragonal) symmetry. In the absence of oxygen vacancies in the second (NNN) coordination sphere, which should take place at low activator (Y^{3+}, TR^{3+}) concentrations, the field symmetry is cubic. In the presence of oxygen vacancies in this coordination sphere, the cubic field of the Y^{3+} (TR^{3+}) ion is strongly distorted and its symmetry substantially decreases. The consideration of interaction with remote coordination spheres leads to additional variations in crystal fields of Y^{3+} (TR^{3+}) and, hence, to the broadening of spectral lines.

4. Raman spectroscopy of the structure of fianites

New procedures for studying Raman spectra of crystals, in particular, at high temperatures were developed by researchers at General Physics Institute, RAS. These procedures were used to investigate structural transformations in crystals of zirconium dioxide solid solutions. Fianites with various stabilising oxides were studied in broad temperature and concentration ranges [11–19].

Raman spectroscopy was used to determine the symmetry, structure, and phase composition of single crystals of cubic $ZrO_2 - Y_2O_3$ solid solutions (8 %–33 %). The disorder of the structure of zirconium dioxide solid solutions is caused, as mentioned above, by the presence of two types of cations Zr^{4+} and Y^{3+} (TR^{3+}) with different valences. The replacement of Zr^{3+} by TR^{3+} leads to the formation of oxygen vacancies. As a result, a part of cations having the eightfold environment in the form of a cube in the fluorite-type lattice will be coordinated with the structure of seven- and six-pointed stars. From the point of view of crystal chemistry, two types of six-pointed stars are usually considered and the possibility of the existence of a coordination smaller than six for Zr^{4+} and TR^{3+} cations is excluded. The concentrations of eight-, seven-, and six-pointed stars will depend on the concentration of the TR_2O_3 impurity and can be calculated based on several variants of the distribution of oxygen vacancies among the anion-sublattice sites.

Experimental data [19] and calculations allow us to explain changes observed in the structure of solid ZrO_2–Y_2O_3 solutions at concentrations of Y_2O_3 between 8 % and 33 %. Three Y_2O_3 concentration regions can be distinguished which correspond to a certain structure of the solid solutions under study.

In the concentration region near the lower boundary of cubic-phase stabilisation (8 %–10 %), irrespective of the type of distribution of vacancies in the lattice, eight-pointed stars dominate, while a part of seven-pointed stars forms defect clusters, which break the translational symmetry, as reflected in Raman spectra.

The most interesting is the region of solid solutions with the concentration of yttrium oxide between 15 % and 20 %. In this concentration range, the lines in X-ray diffraction patterns are narrowed, while the Raman spectrum transforms upon annealing of samples from a broad spectrum inherent in the defect fluorite to a linear spectrum whose intensity is maximal and linewidths minimal for crystals of the $ZrO_2 - 20\ \%\ Y_2O_3$ composition. For the concentration of TR_2O_3 between 15 % and 20 %, eight- and seven-pointed stars dominate. This suggests that in this case the ordered structure of eight- and seven-points can exist. On the other hand, a comparatively large width of spectral lines indicates that the spectrum does not correspond to a stoichiometric compound of a certain composition but only reflects a partial ordering of eight- and seven-pointed stars in the lattice derived from the fluorite lattice.

The increase in the concentration of Eu_2O_3 in $ZrO_2 - Eu_2O_3$ solid solutions above 20 % resulted in the further ordering and formation of the pyrochlore structure. The formation of pyrochlore is caused by the ordering of eight- and six-pointed stars in the absence of seven-pointed stars in the lattice [8]. Based on these studies, the spectrum of ZrO2 – 33 % Eu_2O_3 samples was reliably identified as the spectrum of pyrochlore. The shape of the spectrum depended on the annealing temperature and time. Such a change is typical for the disorder–order phase transition. In [14], the existence of solid solutions with the disordered pyrochlore structure of the $ZrO_2 - (15\ \% - 20\ \%)\ Eu_2O_3$ composition was demonstrated.

For a crystal of the $ZrO_2 - 33\ \%\ Y_2O_3$ composition, such ordering effect is absent. The increase in the Y_2O_3 concentration from 20 % to 33.3 % in $ZrO_2 - Y_2O_3$ solid solutions results in a complete configuration disordering, which is explained by the concentration behaviour of structural elements in the region of the impurity concentration between 20 % and 33 %.

5. Luminescence spectra and lasing properties of fianites

Spectral properties and the possibility of lasing in stabilised zirconium dioxide crystals doped with rare-earth ions have not been adequately studied. The spectral characteristics of TR^{3+} (Eu^{3+}, Nd^{3+}, Er^{3+}) and Cr^{3+} and other transition elements in fianites are presented in [4, 20–26]. It has been found that the optical properties of ZrO_2 crystals with impurities are sensitive to the redox conditions of annealing. All spectroscopic studies of various activators in zirconium dioxide crystals have shown that their broad luminescence bands are inhomogeneous.

In [27], the absorption spectra of the $ZrO_2 - Er_2O_3 - Y_2O_3$ crystals doped with Er^{3+} at different concentrations were investigated at liquid helium temperature. It was found that they consisted of 12 separate groups of lines lying in the spectral region between 30 000 and 4000 cm^{-1}. The absorption spectra considerably changed with changing the Y_2O_3 concentration, which was caused by variations in the environment of the Er^{3+} ion. The absorption lines that are relatively intense at low concentrations of Y_2O_3 can be assigned to spectroscopic centres that have no oxygen vacancies in the nearest coordination sphere. The absorption lines that are intense at high concentrations of yttrium belong to the centres having oxygen vacancies. The absorption lines of Er^{3+} in a $ZrO_2 - Y_2O_3$ crystal are much broader than the lines of rare-earth ions in other matrices.

In [23, 25], the spectral properties of Eu^{3+} ions in ZrO_2 crystals of the tetragonal and cubic modifications were studied. By using the method of polarised luminescence of the Eu^{3+} ion selectively excited by laser radiation, the formation of the environment of this ion in solid ZrO_2–Eu_2O_3 solutions was investigated and the deformation of the local environment caused by the cubic–tetragonal phase transition was determined. It was shown that the symmetry of the environment of cationic sites is formed due to weak tetragonal and rhombic distortions on the initial cubic environment. In [23], the ZrO_2 crystals stabilised simultaneously by Y_2O_3 and Eu_2O_3 were studied; the Eu^{3+} ion was also an activator. In solid $ZrO_2 - Y_2O_3 - Eu_2O_3$ solutions with the tetragonal structure, four types of activating Eu^{3+} centres were distinguished. It was shown that the luminescence spectra of Eu^{3+} can be used to study the phase composition, the formation of structural defects and phase transitions in partially stabilised zirconium dioxide crystals.

In [4, 5], the spectral and lasing properties of ZrO_2–$Y_2O_3 - Nd_2O_3$ crystals were described. Lasing at 1.0609 μm in Nd^{3+} ions was excited by a xenon flashlamp in an elliptical reflector. Laser action was also obtained in Ho^{3+} and Tm^{3+} ions in the $ZrO_2 - Er_2O_3 - Ho_2O_3$ and ZrO_2–

$Er_2O_3 - Tm_2O_3$ crystals. In these solid solutions, Er_2O_3 was simultaneously the stabiliser of the cubic stricture and the sensitiser of Ho^{3+} and Tm^{3+}. Lasing in Ho^{3+} and Tm^{3+} as observed at 2.115 and 1.896 μm, respectively.

Investigations of the spectral properties of zirconium dioxide crystals with various stabilisers and activators have shown that these crystals can be used in tunable lasers because they have broad inhomogeneous luminescence bands. The Yb^{3+} ion featuring a number of important spectral properties may be promising as an activator.

6. Absorption spectra of $ZrO_2 - Yb_2O_3 - Y_2O_3$ fianites

In [1], single crystals of the $ZrO_2-6\,\%\ Yb_2O_3$, $ZrO_2-12\,\%\ Yb_2O_3$, $ZrO_2-20\,\%\ Yb_2O_3$, $ZrO_2-0.3\,\%\ Yb_2O_3-12\,\%\ Y_2O_3$, and $ZrO_2-4\,\%Yb_2O_3-10\,\%Y_2O_3$ compositions were investigated. Because crystals of the first three compositions had a poor optical homogeneity, we studied here in detail only samples containing both Yb_2O_3 and Y_3O_3 oxides.

We studied samples in the form plane–parallel plates. To exclude reabsorption, the luminescence spectra were recorded by using thin ($\sim$ 100 μm) plates. The absorption and luminescence spectra of Yb^{3+} ions were recorded at room and liquid nitrogen temperatures. Luminescence was excited by a laser diode at 970–975 nm and by a tunable colour-centre laser.

Figures 1 and 2 show the absorption spectra of the $ZrO_2-0.3\,\%\ Yb_2O_3-12\,\%\ Y_2O_3$ and $ZrO_2-4\,\%\ Yb_2O_3-10\,\%\ Y_2O_3$ samples. The most intense absorption line of the $ZrO_2 - Yb_2O_3 - Y_2O_3$ crystal is located at 966 nm. The peak absorption coefficient for this line in crystals with the concentrations of Yb_2O_3 equal to 0.3 % and 4 % is 1.63 and 18.44 cm^{-1} and the line half-width is 5.5 and 10 nm, respectively. This absorption line corresponds to the transition between the lower Stark components of the ground and excited levels. The line intensity is more than twice of the intensity of the group of lines in the region of 910 nm, making this line preferable for laser diode pumping. This is also favoured by a large half-width of the line (more than 5 nm), which well corresponds to the half-width ($\sim$ 3 nm) of the emission line of most laser diodes. One can see from Fig. 1 that this line is partially resolved into two components at a low concentration of Yb^{3+} ions (0.3 %). This is explained by the presence of several types of optical centres in the crystal with different local environments. As the concentration of Yb^{3+} ion is increased up to 4 %, a variety of optical centres increases, resulting in the increase in the inhomogeneous broadening of spectral lines. This is demonstrated in Fig. 2, where this line is broadened to 10 nm.

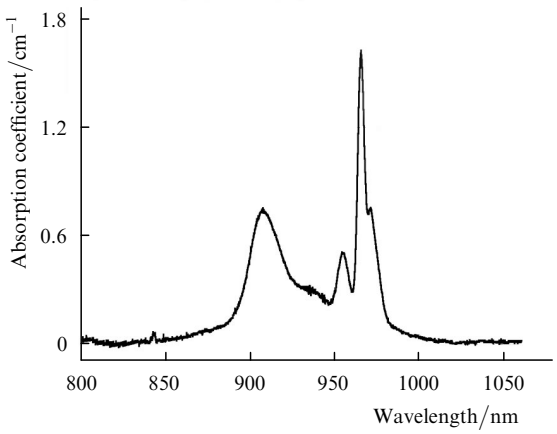

Figure 1. Absorption spectrum of the $ZrO_2-0.3\,\%\ Yb_2O_3-12\,\%\ Y_2O_3$ sample at 300 K.

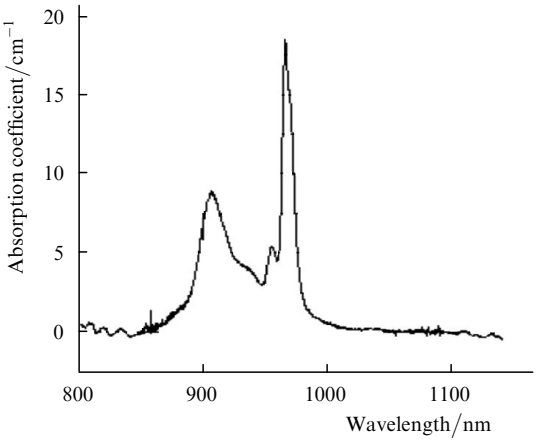

Figure 2. Absorption spectrum of the $ZrO_2 - 4\,\%\ Yb_2O_3 - 10\,\%\ Y_2O_3$ sample at 300 K.

Note that, although the activator concentrations in samples in Figs 1 and 2 differ by more than an order of magnitude, their absorption spectra are similar in respect of the line positions and their relative intensities and differ only in the absolute values of absorption coefficients, which are proportional to the concentration of Yb_2O_3. Such a coincidence of the shapes of absorption spectra for two crystals with different concentrations of Yb^{3+} (0.3 % and 4 %) and approximately the same (14 % and 12.3 %) concentration of the stabiliser safely points to the decisive influence of the total concentration of the stabiliser on the composition of optical centres in the crystal and, hence, on the absorption and luminescence spectra. In this case, the type of a stabiliser (Y_2O_3, Yb_2O_3) weakly affects these characteristics. The activator concentration (0.3 % and 4 %) also plays only a minor role in this respect.

To confirm the assumption that there exist different types of optical centres with different local environments, we investigated absorption spectra at low temperature (20 K). One of these spectra is presented in Fig. 3. One can see that the relative intensities of the lines at 965 and 970 nm at low temperature remain the same as at room temperature, which could not be observed if these lines belong to transitions from different Stark sublevels of one optical centre.

7. Luminescence spectra of $ZrO_2 - Yb_2O_3 - Y_2O_3$ fianites

As in the previous section, the luminescence spectra were studied for two crystals stabilised by two oxides: $ZrO_2-0.3\%\ Yb_2O_3 - 12\%\ Y_2O_3$ and $ZrO_2 - 4\,\%\ Yb_2O_3-10\,\%\ Y_2O_3$. The luminescence spectrum of the first sample is presented in Fig. 4. The luminescence cross section was calculated by the Fuchtbauer–Ladenburg formula. The calculated luminescence cross sections can be considered

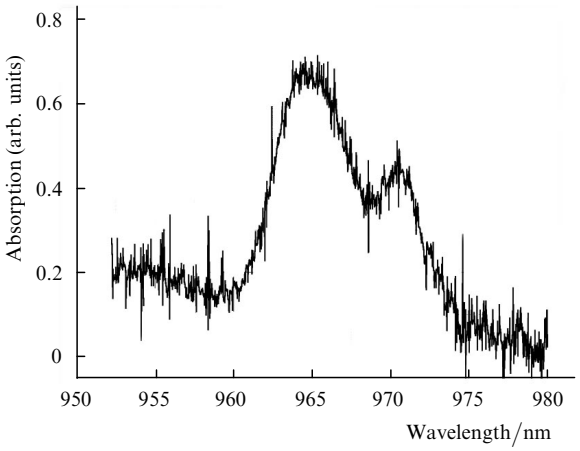

Figure 3. Part of the absorption spectrum of the $ZrO_2 - 0.3\ \%\ Yb_2O_3 - 12\ \%\ Y_2O_3$ sample at 20 K.

only as the upper bound because optical centres of different types in multicentre crystals have different lifetimes, which complicated the application of this formula. The luminescence spectrum presented in Fig. 4 exhibits two bands in the regions 960–980 nm and 1020–1060 nm. The first band obviously corresponds to the $^2F_{5/2} - ^2F_{7/2}$ transition between the lower Stark components of the levels in different Yb^{3+} centres. The second maximum corresponds to transitions from the lower Stark components of the $^2F_{5/2}$ level to the upper components of the $^2F_{7/2}$ ground stste.

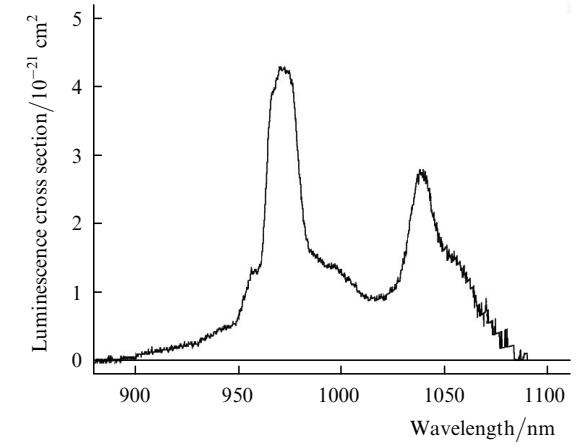

Figure 4. Luminescence spectrum of the $ZrO_2 - 0.3\ \%\ Yb_2O_3 - 12\ \%\ Y_2O_3$ sample.

8. Kinetics of luminescence decay of Yb^{3+} ions in fianites

We present below the data on the luminescence decay for the $ZrO_2 - 0.3\ \%\ Yb_2O_3 - 12\ \%\ Y_2O_3$ and $ZrO_2 - 4\ \%\ Yb_2O_3 - 10\ \%\ Y_2O_3$ fianites excited at different wavelengths. Figure 5 shows the luminescence decay curves for a sample with a low concentration of Yb^{3+} (0.3 %) excited at two wavelengths. The luminescence decay was detected at the short-wavelength luminescence line consisting of several components belonging to different optical centres. Both decay curves are non-exponential. They differ from each other in that upon excitation at 902 nm, long-lived Yb^{3+} centres with the characteristic lifetime $\tau_2 = 1.44$ ms are revealed, while upon excitation at 970 nm, the fraction of short-lived optical centres with the characteristic lifetime $\tau_1 = 0.5$ ms increases. This means that the $ZrO_2 - 0.3\ \%\ Yb_2O_3 - 12\ \%\ Y_2O_3$ crystal has optical centres that differ from each other not only in the positions of absorption and luminescence lines but also in the transition probabilities. This circumstance complicates the measurement of the luminescence cross section by the Fuchtbauer–Ladenburg method.

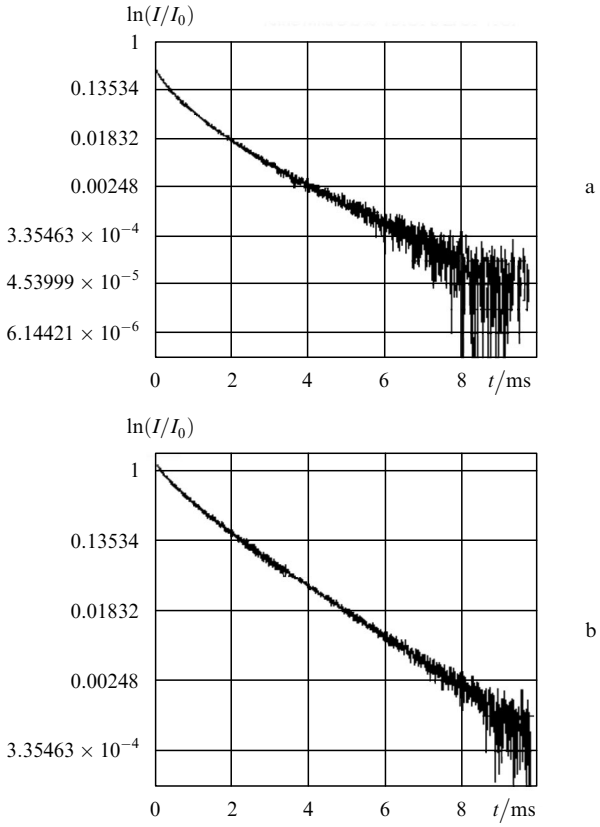

Figure 5. Luminescence decay at 970 nm for the $ZrO_2 - 3\ \%\ Yb_2O_3 - 12\ \%\ Y_2O_3$ sample excited at 970 (a) and 902 nm (b).

The luminescence decay for the $ZrO_2 - 4\ \%\ Yb_2O_3 - 10\ \%\ Y_2O_3$ sample is described by nearly exponential dependence with the decay time 1.3 ms. The difference in the luminescence decay processes can be explained by the increase in the Yb^{3+} concentration leading to energy migration between Yb^{3+} ions. The decay kinetics is almost independent of the excitation wavelength. The luminescence cross section was estimated by using the lifetime $\tau = 1.3$ ms.

9. Selective spectroscopy of $ZrO_2 - Yb_2O_3 - Y_2O_3$ crystals

To verify our assumption about the reason for the non-exponential dependence of the luminescence decay in samples with a low concentration of Yb^{3+}, we recorded and studied the luminescence spectra upon selective excitation. The time-resolved spectra were recorded with a BCI-280 boxcar with a variable temporal window for luminescence recording and the variable window delay with

respect to the excitation pulse. Luminescence was excited by a pulsed tunable colour-centre laser at different wavelength within the inhomogeneous absorption band of Yb^{3+}.

Figures 6 and 7 present the luminescence spectra of a $ZrO_2 - 0.3\,\%\ Yb_2O_3 - 12\,\%\ Y_2O_3$ sample obtained at different excitation wavelengths and different delay times. One can see from Fig. 7b that for a shorter delay time (5 μs), a well-isolated line belonging to short-lived optical centres is observed. As the delay time is increased up to 3 ms, a new line appears which obviously belongs to long-lived centres.

This experiment and also the absorption spectrum of the same sample at 20 K confirm the assumption that the $ZrO_2 - Yb_2O_3 - Y_2O_3$ crystal contains optical centres with different frequencies of transitions between the Stark levels and different probabilities of these transitions.

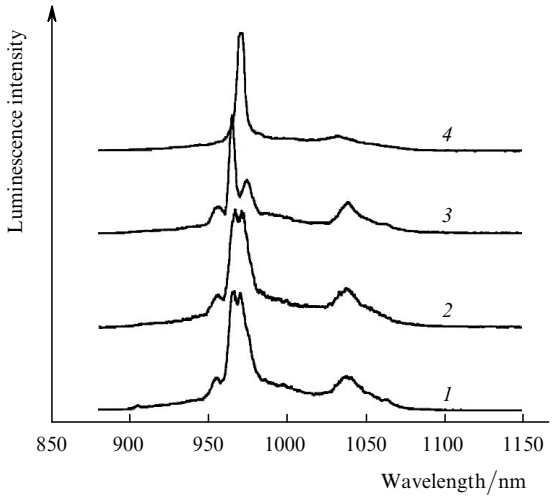

Figure 6. Luminescence spectra of the $ZrO_2 - 0.3\,\%\ Yb_2O_3 - 12\,\%\ Y_2O_3$ crystal at 300 K excited by a colour-centre laser at 902 (*1*), 937 (*2*), 963 (*3*), and 969 nm (*4*). The delay time is $\Delta t = 5$ μs.

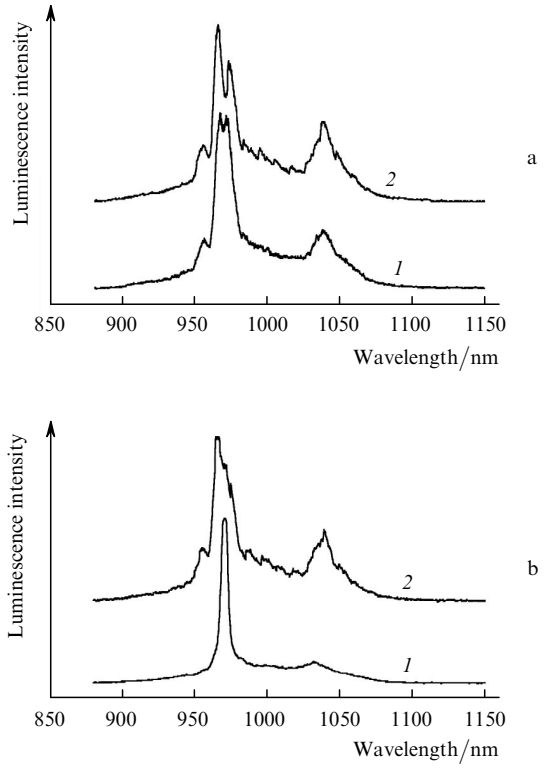

Figure 7. Luminescence spectra of the $ZrO_2 - 0.3\,\%\ Yb_2O_3 - 12\,\%\ Y_2O_3$ crystal at 300 K excited by a colour-centre laser (a) at 937 nm and detected with the delay times $\Delta t = 12$ μs (*1*) and 2 ms (*2*), and (b) excited at 969 nm and detected with time delays $\Delta t = 5$ μs (*1*) and 3 ms (*2*).

10. Gain cross section and lasing of Yb^{3+} in fianites

Figure 8 presents the gain cross sections calculated by using the absorption and luminescence spectra for the radiative lifetime $\tau = 1.3$ ms. The gain line continues far to the long-wavelength region up to 1070 nm. This points to a large Stark splitting of the $^2F_{7/2}$ ground state of the Yb^{3+} ion in the $ZrO_2 - Yb_2O_3 - Y_2O_3$ crystal, which considerably reduces the lasing threshold and makes it possible to tune laser radiation in a broad spectral range.

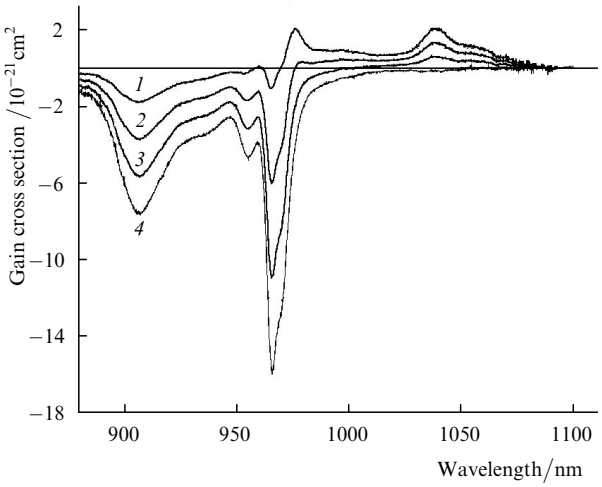

Figure 8. Gain cross sections for the $ZrO_2 - Yb_2O_3 - Y_2O_3$ crystal for the relative inverse population $\beta = 0.75$ (*1*), 0.5 (*2*), 0.25 (*3*), and 0 (*4*).

In [1], lasing experiments were performed with a sample of the $ZrO_2 - 4\,\%\ Yb_2O_3 - 10\,\%\ Y_2O_3$ composition because its absorption coefficient at the pump wavelength is $\sim 20\ cm^{-1}$. Such an active element can be efficiently pumped at a small sample thickness, which provides the miniaturisation of the device. Several active elements of length 1 mm were manufactured from the crystal. The elements were covered by optical coatings of two types.

The AR coating of the first type for the spectral range from 1040 to 1060 nm was deposited on one end of the active element, while another end had a highly reflection (HR) mirror, which was transparent at the pump wavelength. The element with the coating of the second type had a HR mirror for the spectral range 1040–1060 nm on one end, which was transparent at the pump wavelength, and on another end – a mirror transmitting 1 % in the range 960–1060 nm, which provided two passages of the pump radiation.

Pumping was performed by a PUMA, Milon Laser diode array with a fibre pigtail. The output power was 18 W for the fibre diameter equal of 100 μm. Radiation was focused with a $1.5^{\times}$ four-lens objective. The average output

cw power was limited with a shutter with the off-duty ratio 12. Thus, pumping was performed by 4-ms pulses at a pulse repletion rate of 20 Hz. The pump unit was thermally stabilised at 25 °C, which corresponds to the pump wavelength 973 nm.

Figure 9 shows the lasing spectra of the ZrO_2–4 % Yb_2O_3 – 10 % Y_2O_3 crystal obtained with different output mirrors. As the transmission coefficient was changed from 12.5 % to 3.5 %, the lasing wavelength changed from 1041 to 1057 nm. When the active element with the coating of the second types was used, the lasing wavelength was 1060 nm.

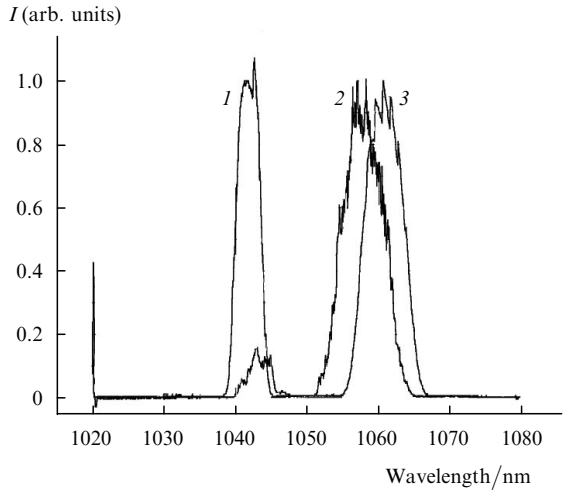

Figure 9. Tuning of the $ZrO_2 - Yb_2O_3 - Y_2O_3$ laser with the output mirrors transmitting 12.5% (*1*) and 3.5% (*2*) and the active element with the second-type coating (*3*).

Figure 10 presents the dependence of the output power on the pulsed pump power for the active element with the coating of the second type. The lasing efficiency in this regime was 44 %, the maximum average power was 415 mW (the maximum pulse energy was 20 mJ) at the laser wavelength 1060 nm, and the lasing threshold was 4 mJ.

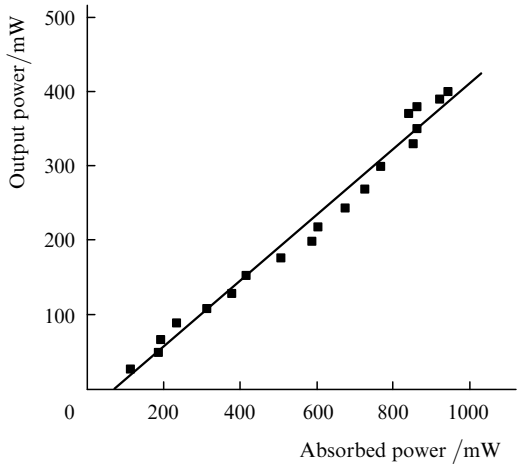

Figure 10. Dependence of the output power of the ZrO_2–4 % Yb_2O_3 – 10 % Y_2O_3 laser on the absorbed pulsed pump power for the slope efficiency $\eta = 44$ %.

The maximum average pulsed power in active elements with the first-type coating was 320 mW at 1042 nm and the laser pulse energy was 16 mJ.

11. Conclusions

We have shown that the shapes of absorption spectra of two crystals with molar concentrations of Yb^{3+} equal to 0.3 % and 4 % and approximately the same concentration (14 % and 12.3 %) of the stabilising impurity coincide qualitatively, which points to the decisive influence of the stabiliser concentration on the composition of optical centres in these crystals and, hence, their absorption spectra. The stabiliser type (Y^{3+} or Yb^{3+}) and the activator concentration weakly affect these characteristics.

The results of our study have shown that the $ZrO_2 - Yb_2O_3 - Y_2O_3$ fianite crystals are promising for the use in diode-pumped tunable solid-state lasers.

Acknowledgements. The authors thank Yu.S. Kuz'minov and L.M. Ershova for their help in the preparation of this paper.

References

1. Shukshin V.E. *Candidate Dissertation* (Moscow: GPI, RAS, 2004).
2. Aleksandrov V.I., Lomonova E.E., Maier A.A., et al. *Kratk. Soobshch. Fiz. FIAN*, (11), 3 (1972).
3. Balitskii V.S., Lisitsina E.E. *Sinteticheskie analogi i imitatsii prirodnykh dragotsennykh kamnei* (Synthetic Analogues and Imitations of Natural Precious Stones) (Moscow: Nedra, 1981).
4. Kuz'minov Yu.S., Osiko V.V. *Fianity. Osnovy tekhnologii, svoistva, primenenie* (Fianites: Fundamentals of Technology, Properties, and Applications (Mocow: Nauka, 2001).
5. Kuz'minov Yu.S., Lomonova E.E., Osiko V.V. *Tugoplavkie materially iz kholodnogo tiglya* (Refractory Materials from a Cold Crucible) (Moscow: Nauka, 2004).
6. Voron'ko Yu.K., Vishnyakova M.A., Lomonova E.E., et al. *Neorg. Mater.*, **40**, 1 (2004).
7. Steele D., Tender B.E.F. *J. Phys. Chem.*, **7**, 1 (1974).
8. Veal B.W., McKale A.G., Paulincas A.P. *Physica B*, **150**, 234 (1988).
9. Stupper G., Barnasconi M., Nicoloso N., et al. *Phys. Rev. B*, **59** (2), 797 (1999).
10. Villella P., Conradson S.D., Espinose-Fallen F.J., et al. *Phys. Rev. B*, **64**, 104 (2001).
11. Voron'ko Yu.K., Sobol' A.A., Tsymbal L.I. *Neorg. Mater.*, **34**, 439 (1998).
12. Voron'ko Yu.K., Zufarov M.A., Ignat'ev B.V., et al. *Opt. Spektr.*, **51**, 569 (1981).
13. Aleksandrov V.I., Voron'ko Yu.K., Ignat'ev B.I., et al. *Fiz. Tverd. Tela*, **20**, 528 (1978).
14. Osiko V.V., Voron'ko Yu.K., Sobol A.A., in *Growth and Defect Structure* (Berlin, Heidelberg, New York, Tokyo: Springer, 1984) Vol. 10, pp 37 – 86.
15. Michel D., Perez-Jorba M., Collonques R. *J. Raman Spectr.*, **5** (2), 163 (1976).
16. Perry C.H., Liu D.W., Ingel R.P. *J. Am. Ceram. Soc.*, **68** (8), 184 (1985).
17. Voron'ko Yu.K., Zufarov M.A., Osiko V.V., et al. *Preprint FIAN, No. 64* (Moscow, 1983).
18. Voron'ko Yu.K., Sobol' A.A., Ushakov S.N., et al. *Neorg. Mater.*, **30**, 803 (1994).
19. Voron'ko Yu.G., Gorbachev A.V., Sobol' A.A. *Fiz. Tverd. Tela*, **37**, 1939 (1995).
20. Aleksandrov V.I., Vishnyakova M.A., Voitsitskii V.P., et al. *Neorg. Mater.*, **26**, 1251 (1990).
21. Merino R.I., Orera V.M., Cases R., et al. *J. Phys.: Condens. Mater.*, **3**, 8491 (1991).

22. Merino R.I., Orera V.M., Lomonova E.E., et al. *Phys. Rev. B*, **52** (9), 1650 (1995).
23. Voron'ko Yu.K., Zufarov M.A., Sobol' A.A., et al. *Neorg. Mater.*, **33**, 452 (1997).
24. Voron'ko Yu.K., Zufarov M.A., Sobol' A.A., et al. *Neorg. Mater.*, **32**, 1063 (1996).
25. Voron'ko Yu.K., Zufarov M.A., Sobol' A.A., et al. *Opt. Spektr.*, **81**, 814 (1996).
26. Dexpert-Ghys J., Faucher M., Card P.J. *Solid State Chem.*, **54** (2), 179 (1984).
27. Arashi H. *Phys. Stat. Sol.*, **10** (1), 107 (1991).